DEPARTMENT OF AEROSPACE ENGINEERING
COLLEGE OF ENGINEERING AND TECHNOLOGY
OLD DOMINION UNIVERSITY
NORFOLK, VIRGINIA 23529-0247

INITIALIZATION AND SIMULATION OF THREE-DIMENSIONAL AIRCRAFT WAKE VORTICES

By
Dr. Robert L. Ash, Principal Investigator
Dr. Z.C. Zheng, Project Director

Final Report
For the period ending May 1997

Prepared for
National Aeronautics and Space Administration
Langley Research Center
Attn: Joseph Murray, Mail Stop 128
Hampton, VA 23681-0001

Under
Grant# NAG-1-1437
Fred H. Proctor, Technical Monitor
Vehicle Operations Research Branch
ODURF #124462

Submitted by the
Old Dominion University Research Foundation
P.O. Box 6369
Norfolk, VA 23508-0369

May 1997

DEPARTMENT OF AEROSPACE ENGINEERING
COLLEGE OF ENGINEERING AND TECHNOLOGY
OLD DOMINION UNIVERSITY
NORFOLK, VIRGINIA 23529-0247

INITIALIZATION AND SIMULATION OF THREE-DIMENSIONAL AIRCRAFT WAKE VORTICES

By
Dr. Robert L. Ash, Principal Investigator
Dr. Z.C. Zheng, Project Director

Final Report
For the period ending May 1997

Prepared for
National Aeronautics and Space Administration
Langley Research Center
Attn: Joseph Murray, Mail Stop 128
Hampton, VA 23681-0001

Under
Grant# NAG-1-1437
Fred H. Proctor, Technical Monitor
Vehicle Operations Research Branch
ODURF #124462

Submitted by the
Old Dominion University Research Foundation
P.O. Box 6369
Norfolk, VA 23508-0369

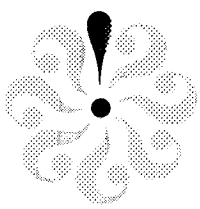

May 1997

Initialization and Simulation of Three-Dimensional Aircraft Wake Vortices

Z. C. Zheng
University of South Alabama, Mobile, AL 36688-0002

AIAA 15th Applied Aerodynamics Conference
June 23-25, 1997, Atlanta, GA

AIAA Paper No. 97-2264

Initialization and Simulation of Three-Dimensional Aircraft Wake Vortices

Z. C. Zheng *
University of South Alabama, Mobile, AL 36688-0002

Abstract

This paper studies the effects of axial velocity profiles on vortex decay, in order to properly initialize and simulate three-dimensional wake vortex flow. Analytical relationships are obtained based on a single vortex model and computational simulations are performed for a rather practical vortex wake, which show that the single vortex analytical relations can still be applicable at certain streamwise sections of three-dimensional wake vortices.

Introduction

Aircraft trailing vortex wakes can cause serious loss of control when following aircraft encounter them. The following aircraft can be subjected to rolling moments which exceed the aircraft's roll control authority, leading to a dangerous loss of altitude, and to possible structural failure. With the advent of large transport aircraft, the wake vortex problem has taken on added significance. Since the probability of an aircraft-vortex encounter is greatest in airports where aircraft operate in close proximity, aircraft spacing at congested airports is dictated by the characteristics of the vortex wakes left in the terminal area[6]. Therefore, prediction of wake vortex trajectories and strengths is especially important for effective airport flight control and maintain maximum traffic volume. Both government agencies (NASA, FAA) and industry (Boeing) feel an urgent need to solve the problem.

In order to fully assess the hazard, complete information is needed regarding such processes as the initial organization of the wake vortex sheet, the subsequent roll-up and generation of primary vortices, the descent and decay of the wake in a real atmosphere, and the response/control characteristics of the encountering aircraft. Since wake vortex trajectories and strengths are altered radically by interactions with the ground plane and by atmospheric conditions, computational simulations have been focused on the viscous interaction between vortex wakes and the ground plane, including atmospheric effects such as stratification, wind shear and turbulence. An in-depth understanding of the mechanisms that bring about wake transport and decay can provide information which could enable the alleviation of airport congestion.

Previously, most computational simulations have been two-dimensional or quasi-two-dimensional (e. g., Ref. 2, 4, 10, 11, 13-17). Those simulations are applicable when the streamwise vortex axial velocity gradients are small comparing with the velocity gradients in vertical and spanwise directions. Two-dimensional simulations can predict the vortex transport behavior at a satisfied level in comparison with measurement data. However, wake vortex decay histories calculated in two-dimensional simulations are questionable. Phenomena such as vortex stretching, vortex bursting or breakdown and Crow instability, which are intrinsically three-dimensional, are unable to be captured using two-dimensional models.

The study will then be concentrated on three-dimensional simulations. Since it is an unsteady problem, flow initialization is required. To specify a physically sound initial three-dimensional wake vortex flow field is always a challenging problem in fluid dynamics, since the roll-up process itself is a complicated phenomenon. However, since only far-downstream flow field is of interest in wake vortex hazard predictions, detailed information of how the vortex is generated on the wing is another research topic and thus excluded in this research. Rather, the initial vortex flow field will be analyzed using integral relationships, instead of detailed complicated CFD approach, although and latter and some experiment data are probably necessary to evaluate the integral model and calibrate some coefficients.

In the three-dimensional algorithms, the upstream in-flow boundary conditions are specified as the initial vortex flow field and thus again it shows the

*Assistant Professor, Mechanical Engineering Department, AIAA Member,

importance of a well-defined initialization. We ran a simulation with uniform axial velocity component (no axial shear) to test the development of the axial flows. Figure 1 is a two-dimensional section of axial velocity contours, with x the axial direction, y and z the lateral and vertical directions, respectively. It shows that a non-physical axial flow field, with half of the axial flow towards the airplane (negative value) and half of it away from the airplane (positive value), has been generated. That means non-practical axial flow initialization can result in incorrect three-dimensional simulations.

Initially, a completely rolled-up wake vortex pair can be modeled as two non-interacting counter-rotating vortices, because of the large separation distance between the two vortices (about eighty percent of aircraft wing span) and the small vortex core radius (about five percent of the wing span). Several azimuthal velocity models have been studied (such as Ref. 7) and most of them are agreeable with measurement data if the model coefficients are properly adjusted. However, the axial velocity component has been of some difficulties to determine, due to lack of systematical measurement data and reliable computational simulations.

There are several researchers who have studied vortex axial velocity after completion of vortex roll-up. Batchelor[3] analyzed the dynamical necessity of axial flow for inviscid vortices: the radial pressure gradient balances the centrifugal force, where any change in the azimuthal motion with distance downstream produces an axial pressure gradient and consequently an axial acceleration. Moore[8] brought viscous effects into the analysis and estimated the axial flow deficit due to the boundary layer on the wing. He concluded that both jet and wake type axial flows could occur depending on the distribution of loading on the wing. Brown[5] showed that axial flow effects of the wing profile drag and lifting system depended on the ratio of profile drag to induced drag. Recently, Rule and Bliss[12] proposed a model based on the Betz method. They obtained a set of ODEs to calculate both tangential and axial velocity profiles.

In spite of the complex of initial axial flows, at the near field (close to the flying aircraft), the profiles of the axial flows can be categorized into three types (in coordinates attached to the aircraft): (1) jet type (excessive to the free stream); (2) wake type (deficit to the free stream); (3) combinations of the two (with jet type close to the vortex center and wake type further away from the center in radial direction). Those profiles are represented in Figure 2. All three types have been observed in flight tests.

Theoretical Analysis

The importance of the axial velocity component in three-dimensional simulation can be explained by a perturbation expression based on two-dimensional formulations, which can be considered as a three-dimensional case with uniform axial velocity. In two-dimensional simulations, the axial direction is converted to time with $t = x/U_o$, where U_o is the flight speed of the aircraft and x is conventionally assigned to axial direction and y and z are spanwise and vertical directions, respectively. Hence, a two-dimensional calculation is actually a steady state three-dimensional calculation with a uniform axial velocity component, which is the flight speed in this case.

Consider the transport equation for the axial component of vorticity, ζ_x, which has the direct contribution to the vortex roll hazard. Strong axial currents occur near the vortex core, where ζ_x concentrates. If we put a small perturbation to the uniform axial velocity, the axial vorticity transport equation becomes:

$$(U_o+u)\frac{\partial \zeta_x}{\partial x} + V\frac{\partial \zeta_x}{\partial y} + W\frac{\partial \zeta_x}{\partial z} = \zeta_x\frac{\partial u}{\partial x} + \zeta_y\frac{\partial u}{\partial y} + \zeta_z\frac{\partial u}{\partial z} + \nu\nabla^2_{yz}\zeta_x\,, \qquad (1)$$

where

$$\zeta_x = \partial W/\partial y - \partial V/\partial z\,,$$

$$\zeta_y = \partial u/\partial z - \partial W/\partial x$$

and

$$\zeta_z = \partial V/\partial x - \partial u/\partial y\,.$$

Substituting the expressions of ζ_y and ζ_z and making use of the continuity

$$\frac{\partial u}{\partial x} + \frac{\partial V}{\partial y} + \frac{\partial W}{\partial z} = 0\,, \qquad (2)$$

Eq. (1) becomes:

$$(U_o+u)\frac{\partial \zeta_x}{\partial x} + \frac{\partial (V\zeta_x)}{\partial y} + \frac{\partial (W\zeta_x)}{\partial z} = -\frac{\partial W}{\partial x}\frac{\partial u}{\partial y} + \frac{\partial V}{\partial x}\frac{\partial u}{\partial z} + \nu\nabla^2_{yz}\zeta_x\,. \qquad (3)$$

Divide the above equation with the constant flight speed and define $u' = u/U_o$, we have

$$(1+u')\frac{\partial \zeta_x}{\partial x}+\frac{1}{U_o}(\frac{\partial (V\zeta_x)}{\partial y}+\frac{\partial (W\zeta_x)}{\partial z})$$
$$=-\frac{\partial W}{\partial x}\frac{\partial u'}{\partial y}+\frac{\partial V}{\partial x}\frac{\partial u'}{\partial z}+\frac{\nu}{U_o}\nabla^2_{yz}\zeta_x\,. \qquad (4)$$

Equation (4) is an exact equation for axial vorticity component. For analytical study purpose, here we assume that the axial flow deviation is small comparing with the flight speed, i.e., $u' \ll 1$. The equation that we obtain is

$$\frac{\partial \zeta_x}{\partial x}+\frac{1}{U_o}(\frac{\partial (V\zeta_x)}{\partial y}+\frac{\partial (W\zeta_x)}{\partial z})$$
$$=-\frac{\partial W}{\partial x}\frac{\partial u'}{\partial y}+\frac{\partial V}{\partial x}\frac{\partial u'}{\partial z}+\frac{\nu}{U_o}\nabla^2_{yz}\zeta_x\,. \qquad (5)$$

Now consider a single vortex case. We integrate Eq. (5) throughout each $y-z$ section, noticing that the area integration of axial vorticity is the total circulation at that section. It can be shown that the resultant equation for the total circulation (at certain x location) is:

$$\frac{d\Gamma_\infty}{dx}=\int_A(-\frac{\partial W}{\partial x}\frac{\partial u'}{\partial y}+\frac{\partial V}{\partial x}\frac{\partial u'}{\partial z})dA\,. \qquad (6)$$

All the integrations of the convection terms (in conservative forms) and diffusion terms are zero, due to the fact that the axial vorticity and its derivatives are zero at the infinite boundary. We also note that Eq. (6) reduces to Betz's first invariant[7] if the axial velocity component is uniform in $y-z$ plane and x is replaced by t/U_o. That is, for two-dimensional single vortex cases, $d\Gamma_\infty/dt=0$.

For the single vortex case, axi-symmetry can be assumed. Using cylindrical coordinates, Eq. (6) becomes:

$$\frac{d\Gamma_\infty}{dx}=-\int_A\frac{\partial V_\theta(r,x)}{\partial x}\frac{\partial u'(r,x)}{\partial r}dA\,, \qquad (7)$$

where V_θ is the tangential velocity of the vortex. Since we are trying to deduce the qualitative influence of the axial velocity profile on the vortex decay behavior, here we choose Rankine vortex to derive a theoretical relationship, without losing generality. In Rankine vortex,

$$V_\theta=\frac{\Gamma_\infty}{2\pi r_c^2}r\,, \qquad (8)$$

when $r\le r_c$, where r_c is the radius of the vortex core. Outside the vortex core, V_θ follows potential vortex velocity distribution. Since most of the axial velocity deviation is inside the vortex core, both u' and $\partial u'/\partial r$ are approximated to be zero outside the vortex core. Substituting Eq. (8) into Eq. (7), we have

$$\frac{d\Gamma_\infty}{dx}=-\int_0^{r_c}\frac{d}{dx}(\frac{\Gamma_\infty}{r_c^2})\frac{\partial u'}{\partial r}r^2dr\,. \qquad (9)$$

After integration by parts and re-arrangement, we obtain

$$\frac{d\Gamma_\infty}{dx}=\frac{-4\Gamma_\infty/r_c^3\int_0^{r_c}u'rdr}{1-2/r_c^2\int_0^{r_c}u'rdr}\frac{dr_c}{dx}\,. \qquad (10)$$

It can be seen that the relationship between total circulation decay and the vortex core size change is depending on the axial velocity inside the core.

If the axial flow is wake type ($u'<0$), when the circulation decreases, the core radius decreases. If the axial flow is jet type ($u'>0$), the numerator in the fraction at the right-hand side of Eq. (10) is negative, while the denominator is still positive for $u'<1$. Thus, when the circulation decreases, the core radius increases.

Then we look at the relationship between maximum tangential velocity and the vortex core under the influence of axial velocity. Substitute the expression

$$\Gamma_\infty=2\pi r_c V_{\theta max} \qquad (11)$$

into Eq. (10), we can have:

$$r_c\frac{dV_{\theta max}}{dx}=\frac{dr_c}{dx}V_{\theta max}(-\frac{1+\frac{2}{r_c^2}\int_0^{r_c}u'rdr}{1-\frac{2}{r_c^2}\int_0^{r_c}u'rdr})\,. \qquad (12)$$

Since $u'<1$, the term in the parenthesis at the right-hand side of Eq. (12) is always negative. Therefore, change of maximum tangential velocity is always in the opposite sense of change of vortex core radius, regardless what type of the axial velocity profiles (jet or wake). When the vortex core grows, the maximum tangential velocity decreases, which is the same case as in two-dimensional single vortex.

In Rankine vortex, the vorticity of the vortex can be written as

$$\zeta_x=\frac{\Gamma_\infty}{\pi r_c^2} \qquad (13)$$

for $r\le r_c$ and $\zeta_x=0$ for $r>r_c$. Substituting Eq. (13) into Eq. (10), we have

$$\frac{d\zeta_x}{dx} = -\frac{2\zeta_x}{r_c}\left(\frac{1}{1-\frac{2}{r_c^2}\int_0^{r_c} u' r dr}\right)\frac{dr_c}{dx} . \qquad (14)$$

Again, note that the denominator in the parenthesis at the right-hand side of Eq. (14) is positive for any $|u'| < 1$. That means when the vortex core grows, the vorticity inside the vortex core decreases, so does the maximum tangential velocity as shown in Eq. (12).

It should be noted that the above relationship (i.e. Eqs. (10), (12) and (14)) is valid under the condition that $u' \ll 1$ for a single vortex. However, it offers a guide line to estimate the influence of axial velocity profile.

Computational Model

In realistic wake vortex simulation for airport traffic control purpose, several effects have to be included, such as interactions between a pair of vortices in the fully rolled up aircraft wake and the ground and the terminal area atmospheric conditions. The computational model used in this research is based on the NASA TASS (Terminal Area Simulation System) computational program.

The code uses Arakawa[1] C-type grid and is conservative quadratically. Meteorological phenomena, such as atmospheric turbulence and stratification effects are well embedded in the computational model. The Smagorinsky sub-grid scale model is used for the large-eddy turbulence simulation. The readers are referred to the two references by Proctor[9,10] for the details of the numerical model. Some features are briefly stated here. The equations are in primitive variables for time dependent, compressible flows. The explicit scheme uses 4th-order central difference on staggered, uniform grid in space, with time-split march on acoustically active terms and non-acoustical terms. The time march step is dynamically calculated for each time march to satisfy stability conditions.

Initially we put the vortex pair high above the ground and the separation between the vortices is large. Therefore during early time period, the vortex behaves similar to a single vortex. In stead of Rankine type vortex model, the following vortex model is chosen, to be compatible with others in the wake vortex simulations[10]:

$$V_\theta = \frac{\Gamma_\infty}{2\pi}\frac{r}{r_c^2 + r^2} . \qquad (15)$$

The axial velocity profiles are set as:

$$u' = \pm u'_{max} exp(-cr^2/r_c^2) , \qquad (16)$$

where + and − is corresponding to jet and wake type axial flows and c is a axial flow spreading coefficient in radial direction. In the test cases here we chose $u'_{max} = 0.1$ and $c = 10$.

As mentioned previously, the computation is for unsteady, three-dimensional simulations. If the case reaches steady state, then the time march is considered as pseudo-time march. The steady-state convergence criterion used is 10^{-3} drop of residue for all velocity and pressure (although in most cases the steady state is hard to reach). The initial condition is started with two single vortices (Eq. (15)) with axial velocity (Eq. (16)). That initial condition is stacked for about 20 percent of the total length of the domain in axial direction. Then the inflow boundary condition is kept as the same as what initially specified (at the upstream end of the domain). Both the top boundary and downstream-end boundary are open boundaries. The bottom boundary is specified as ground boundary and no-slip boundary conditions are used.

The initial circulation and flight speed are $550m^2/s$ and $61.75m/s$, respectively, which are close to a DC-10 vortex wake. The initial r_c is chosen as $7m$. The initial height from the ground and separation between the two vortices are $70m$ and $50m$, respectively. The grid sizes are $1.75m$ in $y-z$ plane and $4m$ in axial direction. The Smagorinsky turbulence model is turned off in the current runs, by using a very small coefficient with the term so that the viscous effect is mostly from the molecular viscosity.

Two test cases are shown in the following, one with a wake type axial velocity profile and the other with a jet type. Since the crosswind effects are not included, the flow is symmetric in spanwise direction, thus only half of the flow field needs to be calculated. The domain is $640m$ in axial (x) direction, $52.5m$ in spanwise (y) direction and $104m$ in vertical (z) direction. The time march is stopped at 0.3 minute and steady state solution is not reached, according to the convergence criterion specified. That is probably because the separation near the ground is a unsteady phenomenon, which we do not include in the discussion in this paper.

Figure 3 is the $x-z$ plane wake-type axial velocity contours at $y = 25m$ (about the position of the center of the vortex), which shows the propagation history for the axial velocity profile at 0.1,

0.2 and 0.3 minutes. It can be seen that at 0.1 minute, the profile reaches about $61.75m/s \times 6s = 370.5m$. At 0.2 minute, the profile is supposed to reach $61.75m/s \times 12s = 741m$, which is larger than the domain size. Then at 0.3 minute, the flow field is more established than at 0.2 minute and we chose that time level to analyze the flow field, although the steady state solution is not reached as explained. The same propagation type is found in the case specified with jet-type axial velocity profile.

In both cases, the maximum vorticity at the vortex center decreases and the vortex core size increases, in agreement with Eq. (14). The vortex core size is determined from the span-wise velocity (v) contours. Since the vortex has a downward motion due to interactions between the two vortices in the vortex pair, vertical velocity component is not a good measure for vortex core size. The distance between the zero span-wise velocity contour and the minimum contour (the largest negative value) is used as the vortex core radius. We consider that way of quantifying the vortex cores reducing the influences from both the mirror vortex and the ground plane. Figure 4 shows the $y-z$ section contours of x-direction vorticity and the v-velocity component at the first x plane, which is the same for both wake and jet cases. Figure 5 is for the wake case at the last x plane and Figure 6 is for the jet case at the same plane. Note that the v contours and x-vorticity contours are not exactly at the same x location, because of the staggered grid used in the computation. It can be seen that the maximum vorticity level decreases about 15.2% and the core size increases about 13.3% in the wake case, while in the jet case the maximum vorticity level decreases about 17.9% and the core size increases about 6.7%. In general, those two cases do not show significant difference. We expect that if the domain size is longer in the axial direction, more difference will show.

It needs to be pointed out that at certain axial locations, the maximum x-vorticity level does increase a little, accompanied by very little increase in the core size in both jet and wake cases, which is in the opposite trend as predicted by Eq. (14). For example, between 316m and 348m, ζ_x increases from 6.314/s to 6.339/s and the core radius increases from 7.6m to 7.75m in the jet case. In the wake case, between 388m and 420m, ζ_x increases from 6.4/s to 6.435/s and the core radius increases from 7.6m to 7.8m. However, such small changes can hardly influence the overall vortex behavior.

The total circulation should be used to verify Eq. (10), which is probably more interesting, because the sign of the axial velocity deviation changes the sign of the circulation/core-size relation. However, since the computation includes two vortices as well as the ground plane, total circulation for just one vortex is difficult to calculate and mostly not of interest for practical purpose.

Conclusion

The axial velocity component is important for three-dimensional wake vortex simulations. Initial axial velocity profiles influence the vortex decay behavior. Analytical relationships for small axial velocity deviation have been developed in single vortex cases. Those results show that the sign of the axial velocity deviation can change the relation between the total circulation and the vortex core size, but not the relations between vorticity, maximum tangential velocity, and the core size change.

Computational simulations were tested for both jet and wake type axial flow, with minimal influence from the ground and the mirror vortex in the wake vortex pair. Not surprisingly, the computational results are in agreement with the trend predicted in the analytical studies for the relationship between vorticity and core size, although at some locations opposite trend is detected with negligible influence on the overall vortex decay. The relationship for the total circulation needs to be validated using different simulation setup. For future research, the influence of strong axial currents, instead of small deviations, should be studied.

Acknowledgement

This research was under the support of NASA research grants NAG1-1437 and NAG1-1911, both from the NASA Langley Research Center. Dr. F. H. Proctor is the technical monitor. The author would thank Mr. K. Baek at U. of South Alabama for the help of post-processing some results.

References

1. Arakawa, A. 1966 "Computational Design for Long-Term Numerical Integration of the Equations of Fluid Motion: Two-Dimensional Incompressible Flow, Part I.", *J. Comp. Phys.*, Vol 1, 119-143

2. Ash, R. L. and Zheng, Z. C. 1996 "Numerical Simulations of Commercial Aircraft Wakes Subjected to Airport Surface Weather Conditions", *34th AIAA Aerospace Sciences Meeting and Exhibit*, Reno, NV., AIAA Paper No. 96-0660.

3. Batchelor, G. K. 1964 "Axial Flow in Trailing Line Vortices", *J. Fluid Mechanics*, Vol. 20, pp. 654-658.

4. Bilanin, A. J., Teske, M. E. and Hirsh, J. E. 1978 "Neutral Atmospheric Effects on the Dissipation of Aircraft Vortex Wakes", *AIAA J.*, Vol. 16, pp. 956-961.

5. Brown, C. 1973 "Aerodynamics of Wake Vortices", *AIAA J.*, Vol. 11, pp. 531-536.

6. Hallock, J. N. 1992 *Proceedings of the Aircraft Wake Vortices Conference*, Washington, D. C., October 1991, DOT/FAA/SD-92/1.1 and 1.2.

7. Lamb, H. 1945 *Hydrodynamics*, 6th Edition, Dover.

8. Moore, D. W. 1973 "Axial Flow in Laminar Trailing Vortices", *Proc. R. Sco. London* A, Vol. 333, pp. 491-508.

9. Proctor, F. H. 1987 "The Terminal Area Simulation System. Volume I: Theoretical Formulation", NASA Contractor Rep. 4046, NASA, Washington DC.

10. Proctor, F. H. 1996 "Numerical Simulation of Wake Vortices Measured During the Idaho Falls and Memphis Field Programs", *14th AIAA Applied Aerodynamics Conference Proceedings*, Part 2, pp. 943-960, New Orleans, LA, June, 1996, AIAA Paper No. 96-2496.

11. Robins, R. E. and Delisi, D. P. 1990 "Numerical Study of Vertical Shear and Stratification Effects on the Evolution of a Vortex Pair", *AIAA J.*, Vol. 28, pp. 661-669.

12. Rule, J. A. and Bliss, D. B. 1996 "Prediction of Turbulent Trailing Vortex Structure from Basic Loading Parameters", *14th AIAA Applied Aerodynamics Conference Proceedings*, Part 2, pp. 932-942, New Orleans, LA, June, 1996, AIAA Paper No. 96-2495.

13. Zheng, Z. C. 1996 "The Effects of Atmospheric Turbulence on Aircraft Wake Vortices Near the Ground", *27th AIAA Fluid Dynamics Conference*, New Orleans, LA, June, 1996, AIAA Paper No. 96-1954.

14. Zheng, Z. C. and Ash, R. L. 1996 "A Study of Aircraft Wake Vortex Behavior Near the Ground", *AIAA Journal*, Vol. 34, No. 3, pp. 580-589.

15. Zheng, Z. C., Ash, R. L. and Greene, G. C. 1994 "A Study of the Influence of Cross Flow on the Behavior of Aircraft Wake Vortices Near the Ground", *Proceedings of the 19th Congress of the International Council on the Aeronautical Sciences*, Anaheim, CA, Vol. 2, pp. 1649-1659.

16. Zheng, Z. and Ash, R. L. 1993 "Prediction of Turbulent Wake Vortex Motion Near the Ground", *Transitional and Turbulent Compressible Flows*, edited by L. D. Kral and T. A. Zang, ASME Fluids Engineering Conference, Washington, D.C., ASME FED Vol. 151, pp. 195-207.

17. Zheng, Z. and Ash, R. L. 1991 "Viscous Effects on a Vortex Wake in Ground Effect", *Proceedings of the Federal Aviation Administration International Wake Vortex Symposium*, Washington, D.C., pp. 31-1-31-30.

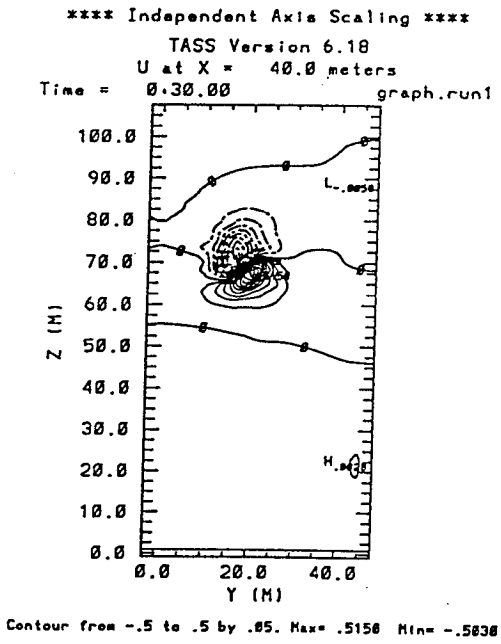

Figure 1: 2D Section of Axial Velocity Contours

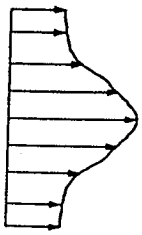

(1)

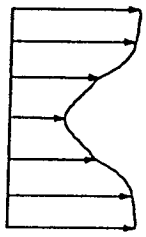

(2)

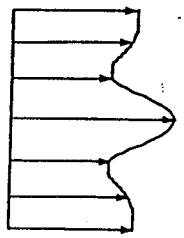

(3)

Figure 2: Axial velocity profiles

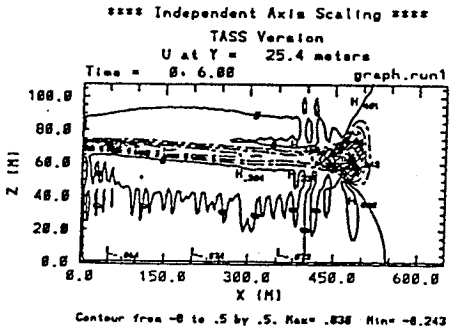
**** Independent Axis Scaling ****
TASS Version
U at Y = 25.4 meters
Time = 0. 6.00
graph.run1
100.0
80.0
60.0
40.0
20.0
0.0
Z (M)
0.0
150.0
300.0
450.0
600.0
X (M)
Contour from -0 to .5 by .5. Max= .838 Min= -0.243

(a)

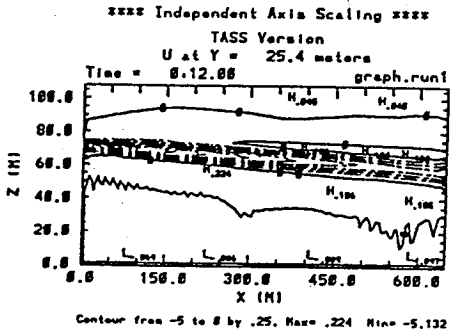
**** Independent Axis Scaling ****
TASS Version
U at Y = 25.4 meters
Time = 0.12.00
graph.run1
100.0
80.0
60.0
40.0
20.0
0.0
Z (M)
0.0
150.0
300.0
450.0
600.0
X (M)
Contour from -5 to 0 by .25. Max= .224 Min= -5.132

(b)

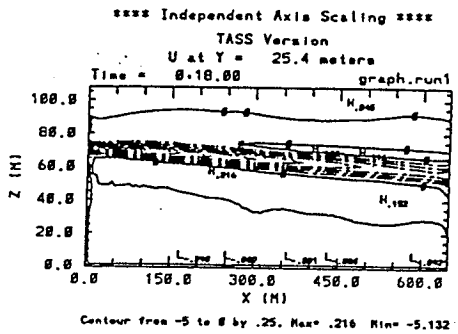

(c)

Figure 3: Axial velocity development at: (a) t=0.1 min., (b) t=0.2 min., (c) t=0.3 min.

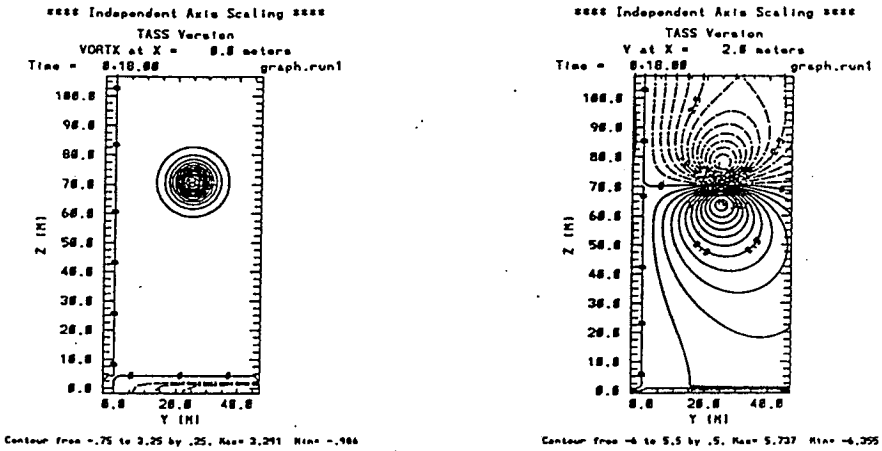

(a) (b)

Figure 4: (a) Axial vorticity (b) Span-wise velocity contours at the first axial plane

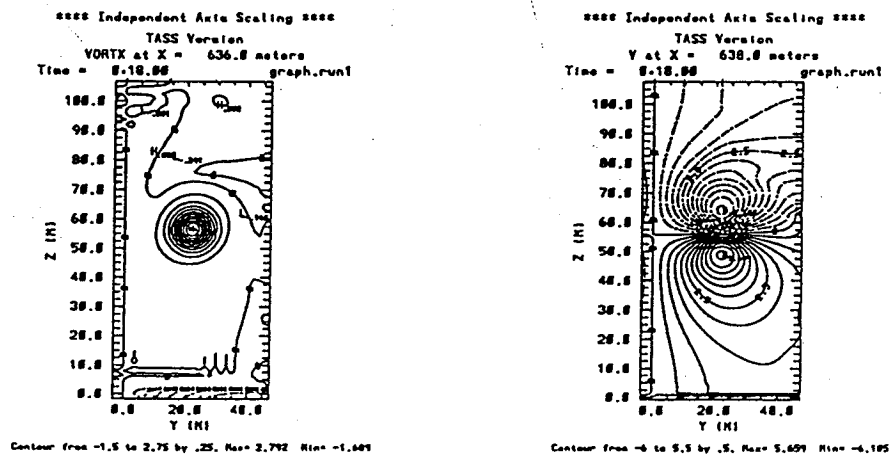

(a) (b)

Figure 5: (a) Axial vorticity (b) Span-wise velocity contours at the last axial plane in the wake case

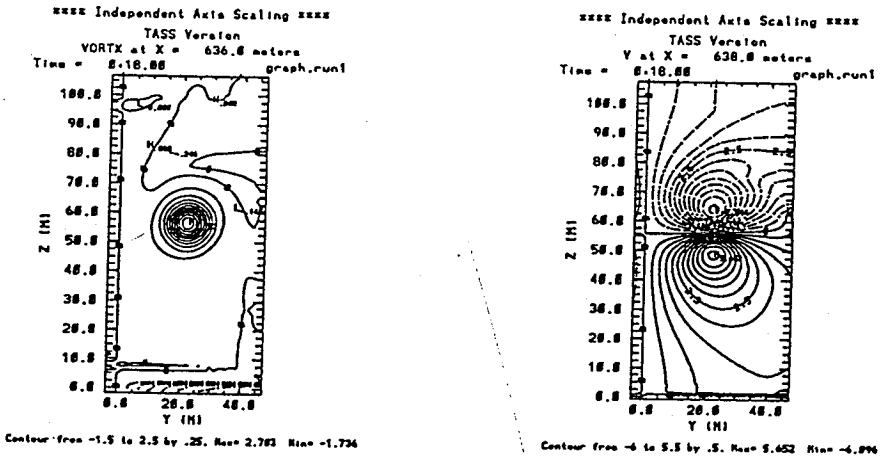

(a) (b)

Figure 6: (a) Axial vorticity (b) Span-wise velocity contours at the first axial plane in the jet case